Available online at www.sciencedirect.com
ScienceDirect
Journal of the European Ceramic Society 32 (2012) 317–324
www.elsevier.com/locate/jeurceramsoc

Strengthening of Vickers indented 3Y-TZP by hydrothermal ageing

F.G. Marro [a,b,*], M. Anglada [a,b]

[a] Dept. of Materials Science and Metallurgical Engineering, Universitat Politècnica de Catalunya, Av. Diagonal 647, 08028 Barcelona, Spain
[b] Center for Research in Nanoengineering, CRnE, Universitat Politècnica de Catalunya, Pascual i Vila 15, 08028 Barcelona, Spain

Received 7 June 2011; received in revised form 28 July 2011; accepted 3 August 2011
Available online 13 September 2011

Abstract

The effect of hydrothermal ageing on indentation cracks has been determined in 3Y-TZP by measuring the flexure strength of indented specimens before and after ageing. A substantial increase in strength was observed after ageing, in contrast to the well known decrease in strength in smooth specimens with only natural flaws. The increase in strength with ageing also occurs if the indentation residual stresses are previously removed by annealing. Observations around the crack tip show the formation of a highly microcracked zone during vapour exposure. Fractographic and micro-Raman analysis observations show that the profile of the cracks is marked on the fracture surface by this zone which is intergranular with a crumbled appearance and in which transformation has taken place. The increase in strength is discussed in terms of crack tip blunting induced by the multiaxial stresses that develop in front of the crack under bending.

Keywords: ZrO_2; Fracture; Mechanical properties; Strength; Toughness and toughening

1. Introduction

Tetragonal polycrystalline zirconia stabilized with 3% mol yttria (3Y-TZP) has been used in orthopaedics for years and, more recently, in a large range of dental devices (crowns, bridges, abutments and implants).[1] These applications arise from its good biocompatibility and high mechanical strength of ~1000 MPa. Additionally, it possesses a moderate fracture toughness of ~5 MPa $m^{1/2}$ caused by a phase transformation mechanism from tetragonal (t) to monoclinic (m) in front of a propagating crack. This locally induced t–m transformation is accompanied by a volume increase of about 4% which shields the crack tip as it extends.[2] On the other hand, the t–m transformation can also spontaneously nucleate at the surface during exposure to humid environment at temperatures between 25 and 300 °C.[3] With time, it extends into the bulk accompanied by micro-cracking, resulting in a loss of mechanical integrity in the affected surface. TZP ceramics stabilised with different type of aliovalent cations are susceptible, in a variable degree, to this phenomenon which is frequently referred to as low temperature degradation (LTD).[4] This lack of long term stability is a serious drawback for applications in humid environments. LTD has been detected in some explanted femoral heads made of 3Y-TZP after a few years *in vivo*. In this case, LTD may cause roughening of the surface[5,6] and grain pull out under contact loading inducing osteolysis and aseptic loosening.[7]

LTD reduces the strength of a TZP ceramic because of the formation of low toughness monoclinic content and microcracks at the affected surface.[8–12] As strength is controlled by the defect population, it is important to assess the effect of hydtrothermal ageing on cracks. For this purpose, one has to consider the strength of specimens with artificial cracks larger than the natural flaw population. Indentation cracks are an important tool for this study because they are sharp, easy to produce and, if sufficiently large, they become the critical defect. In 3Y-TZP, indentation cracks are frequently of Palmqvist type (i.e., not connected below the imprint) with a shape that depends on the specific indentation load.[13]

To the best of our knowledge, there exists only one work on the effect of ageing[14] on Vickers indented 3Y-TZP by Wang et al. in 1992, who surprisingly report a partial recovery of strength with ageing of the indented specimens in coarse grain size (1.2 μm) 3Y-TZP. However, a close examination of their results shows that the scatter of strength for all conditions practically

* Corresponding author at: Center for Research in Nanoengineering, CRnE, Universitat Politècnica de Catalunya, Pascual i Vila 15, 08028 Barcelona, Spain. Tel.: +34 93 40 54454.
E-mail address: fernando.garcia.marro@upc.edu (F.G. Marro).

0955-2219/$ – see front matter © 2011 Elsevier Ltd. All rights reserved.
doi:10.1016/j.jeurceramsoc.2011.08.019

overlap each other, so their results are not conclusive, and neither do they show any fractography observation of the tested specimens. Besides this single study, in the past the attention has been focussed on the influence of ageing on the strength of specimens with natural flaws without paying attention to the precise effect on surface cracks. The present work studies the effect of LTD on the strength of specimens with indentation cracks. Some indented specimens were annealed with the purpose of removing the indentation residual stresses. By doing so, it is also important to minimise any possible crack healing or blunting during the high temperature annealing treatment. All these points are addressed here, as well as the change in strength during hydrothermal ageing of cracked specimens.

2. Materials and procedures

The specimens consisted in 3Y-TZP cylindrical rods (8 mm diam., 64 mm length) from Kyocera Corporation (Japan). The microstructure and mechanical properties of this ceramic are reported elsewhere.[15,16] The Vickers hardness measured with 1 kg load is HV1 = 12.5 GPa and the average grain size is 0.30 μm.

2.1. Fracture toughness

The fracture toughness was estimated by the indentation method. Discs cut from the rods were polished with colloidal silica up to mirror-like finishing; then indented in a range of loads between 5 and 40 kg producing cracks at the imprint corners. The indentation fracture toughness K_{IC}^{ind} was then obtained with the expression proposed by Niihara et al.[17] for Palmqvist cracks:

$$K_{IC}^{ind} = 0.025\left(\frac{E}{H}\right)^{0.4}\left(\frac{PH}{8c}\right)^{1/2}; \quad 1 \le \frac{2c}{d} \le 2.5 \qquad (1)$$

Here, P is the indentation load, d the semi-diagonal of the imprint, $2c$ is the crack length at the surface as measured from the indentation vertex to the crack tip, and the hardness parameter stands for $H = P/2d^2$. Eq. (1) implies that the crack length increases linearly with the indentation load and the slope of such a representation allows determining the indentation fracture toughness. Here, this fit (Fig. 1) yields a value of 5.2 MPa $m^{1/2}$. Due to the limitations of the indentation method, there are uncertainties whether it gives the correct fracture toughness for a specific material.[18] However, in small grain size standard 3Y-TZP the method yields reasonable values as compared to more rigorous methods.[19] The existence of R-curve behaviour is neglected since for small grain size 3Y-TZP the increase in resistance to crack growth is relatively small and it takes place only at very short crack extensions.[20]

2.2. Strength evaluation

The rods were indented on the surface with a 10 kg load. The Palmqvist cracks induced at the imprint corners were roughly semi-elliptical, with the larger semi-axis denoted by a in the depth direction and the shorter one at the surface and denoted by c with $a/c \approx 1.9$. Some of the indented rods were hydrothermally aged at 131 °C in water vapour in autoclave pressurised at 2 bars for different periods of time. The surface of the specimen transformed from tetragonal to monoclinic; the thickness of the degraded surface layer changed from values similar to the grain size after a few hours of hydrothermal ageing to up about 10–12 μm after about 200 h.[15]

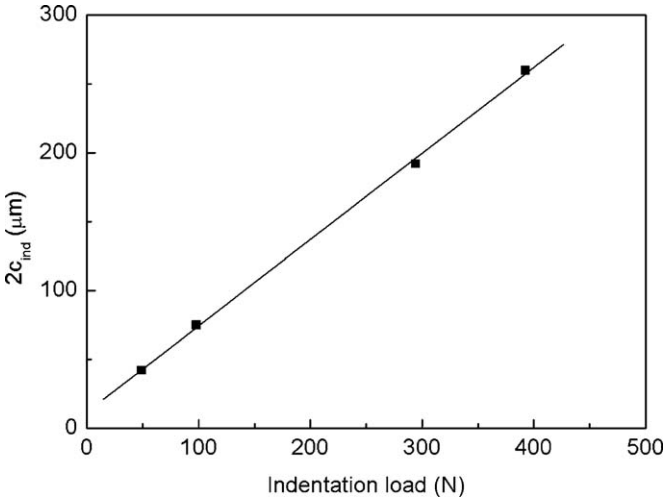

Fig. 1. Increase of the crack length with indentation load in discs obtained from the as received ceramic (slope of the linear regression allows estimating fracture toughness with the method of Niihara et al.[17]).

In order to remove the indentation residual stresses, some of the indented rods were annealed at 1200 °C, since this temperature is commonly used in TZP zirconia to remove surface deformation as well as to reverse any monoclinic phase to tetragonal.[21] The effect of this annealing on the indentation residual stresses was then assessed. Rods indented with 5 kg load were annealed for different periods of time and their flexural strength was determined. It was observed that the strength of the indented rods increases for annealing times of up to 1 h (see Fig. 2), while the strength does not practically change any

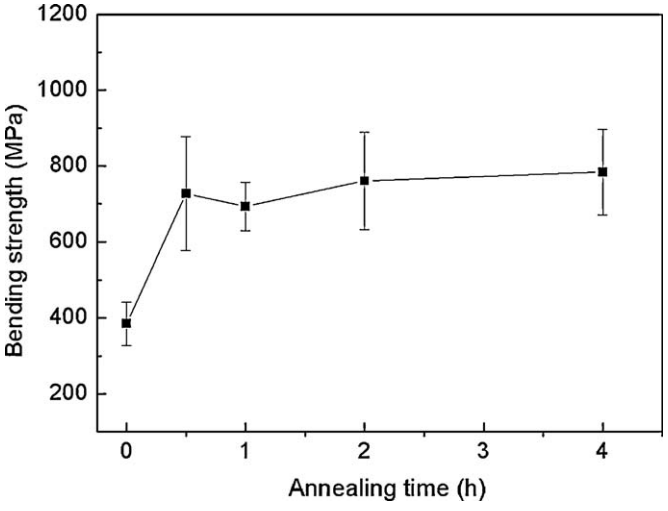

Fig. 2. Strength recovery with annealing of indentation cracks. Each data point corresponds to the average strength of ten rod specimens indented with a 5 kg load and then annealed for a certain period of time.

further for longer times. Therefore, this was the time selected for all further annealing treatments.

The rods will be referred to as "I" (only indented), "I + A" (indented + annealed), "I + D" (indented + degraded) and "I + A + D" (indented + annealed + degraded). The strength of all the specimens was assessed by four point bending with support and loading spans of $l = 60$ mm and $l_i = 30$ mm, respectively. The load was applied at a rate of 200 N/s in a servo-hydraulic testing machine Instron 8511. Maximum tensile stress at the surface was calculated from the maximum applied load F with the following expression:

$$\sigma = \frac{8F(l - l_i)}{\pi D^3} \quad (2)$$

Initially, the fractured surfaces were observed by laser scanning confocal microscopy (LSCM, Olympus Lext); further detailed fractography was carried out by scanning electron microscopy (SEM, Jeol JSM 6400). Atomic force microscopy in tapping mode (AFM, Veeco Dimension) was also performed on some of the degraded specimens in order to evaluate at the smallest possible scale local changes at the affected surface.

2.3. Monoclinic content evaluation

The phase-transformation mechanism was assessed by micro-Raman spectroscopy on the fracture surface of a Palmqvist crack exposed to hydrothermal exposure. Spectra were collected with a triple monochromator spectrometer T64000 (Horiba/Jobin-Yvon) with a coupled CCD detector cooled with liquid nitrogen. The source of excitation was an Argon-ion laser Innova 300 (Coherent Laser Group) at 514 nm wavelength. The spectrum integration time was 60 s with averaging the recorded spectra over two successive measurements. The laser beam was focused using an optical microscope with 100× long-focal objective (lateral resolution of ~1 μm) while a monitor screen connected to the microscope allowed exploring the sample and recording the spectra from the surface on the residual imprints. All spectra were baseline corrected before determining the intensity of the bands. The monoclinic volume fraction was estimated as follows[22]:

$$V_m = \frac{{I_m}^{181} + {I_m}^{190}}{2.2{I_t}^{147} + {I_m}^{181} + {I_m}^{190}} \quad (3)$$

Here, I_m and I_t represent the intensities of the monoclinic and tetragonal bands respectively; the super-indexes identify the Raman shift in cm^{-1} units.

3. Results

3.1. Strength of indented specimens

The reduction in strength of indented specimens (I) as a function of the indentation load was determined (Fig. 3). The same tests on annealed specimens (I + A) showed that their strength was about 60% higher because of the absence of indentation residual stresses. In ceramics with half-penny indentation cracks and without R-curve, the strength should fall with indentation load following[23] a dependence $\sigma \propto P^{-1/3}$. However, if the cracks are of Palmqvist type and Eq. (1) is valid, then this dependence should be of the type $\sigma \propto P^{-1/2}$. In order to determine the exact dependence for the present cracks, an expression of the type $\sigma \propto P^b$ was fitted to the strength of both I and I + A specimens in the range between 5 and 40 kg (where Eq. (1) holds). The fitting for both conditions yielded exponents very close to 0.5, $b = -(0.48 \pm 0.01)$ and $b = -(0.55 \pm 0.07)$ for I and for I + A specimens, respectively. This further confirms the suitability of Eq. (1) for describing the change in residual stress intensity factor of Palmqvist cracks in the range of indentation loads studied. Additionally, the correct fitting of the reduction of the strength by the above expression indicates that the data is not influenced by the existence of an R-curve. However, the present results do not exclude the existence of crack shielding in only the first few microns of crack extension, as has been reported for 3Y-TZP of small grain size.[20]

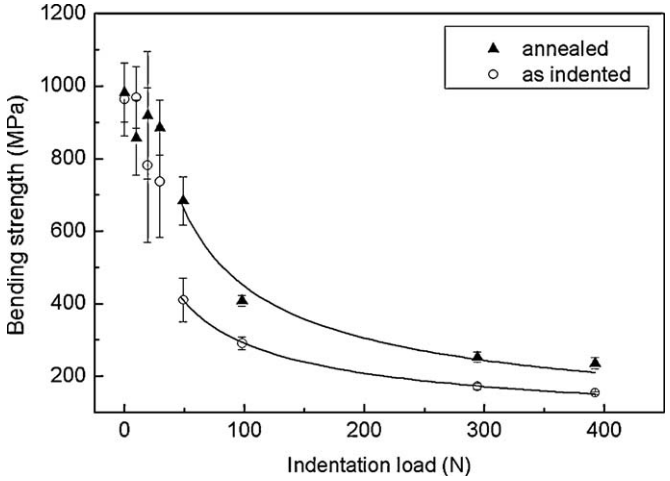

Fig. 3. Strength of I and I + A specimens. The lines correspond to fits of the type $y = ax^b$.

3.2. Strength of indented specimens after ageing

Specimens with a 10 kg indentation were aged for different periods; then the flexural strength was evaluated. After ageing for 50 h, no relevant change in strength was appreciated, but for periods equal or longer than 100 h the strength of I + D specimens increased (Fig. 4). After 200 h, the strength increased more than twice. We focussed our attention on this long ageing period, so that a detailed study was carried out by ageing for 200 h and by using 10 specimens for each condition tested. The observed increase in flexural strength by ageing was confirmed: the strength of I specimens was 291 ± 18 MPa, but after ageing for 200 h it reached 690 ± 32 MPa.

The present ageing temperature is too low compared to the annealing temperature of 3Y-TZP for affecting the indentation residual stresses; however this possibility was not disregarded. Nevertheless, even if residual stresses were somehow relaxed by the hydrothermal exposure, this could not explain the observed rise in the strength. The reason is that when residual stresses are completely removed by annealing, the strength increases only

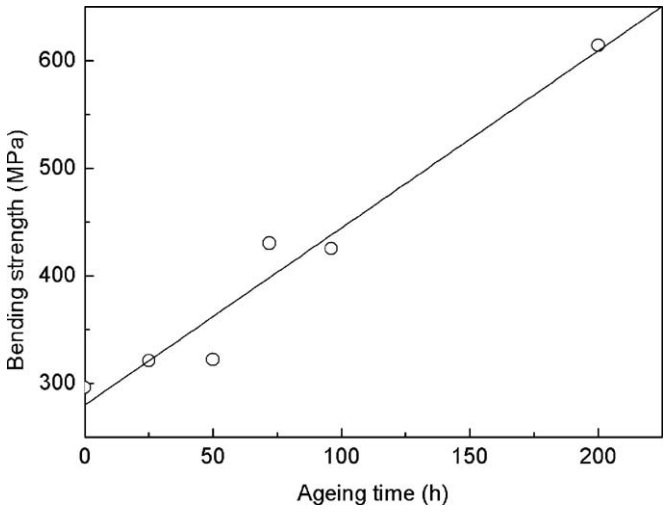

Fig. 4. Strength of indented specimens (I + D) aged for different times.

by 60% ($\sigma_{I+A} = 461 \pm 44$ MPa, see Fig. 5) while the observed increase after hydrothermal ageing is 137% (690 ± 32 MPa as mentioned previously).

Hydrothermal ageing was then performed on specimens with annealed indentation cracks (I + A + D specimens). After annealing, identification of the crack tip is difficult because of partial crack closure; moreover, it was not clear whether annealing may actually join the crack faces preventing the interaction of water vapour with the closed crack face during ageing. However, as it will be shown below, the strength of I + A specimens is in reasonable agreement with the value expected by assuming that no welding of the crack faces took place during annealing. Even more significant, the I + A + D specimens were also strengthened with respect to I + A specimens (Fig. 5). Since the indentation residual stress had been removed by high temperature annealing before ageing, an explanation based on removal of residual stresses cannot alone account for the observations.

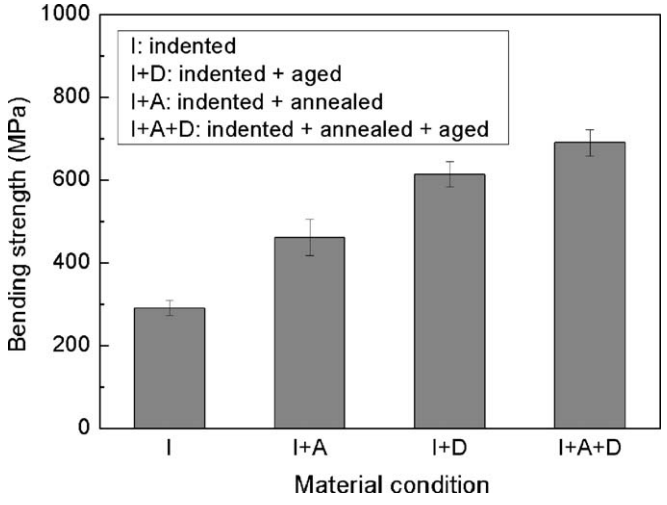

Fig. 5. Strength of specimens under different treatments: as indented ("I"), after annealing ("I + A"), after hydrothermal exposure of 200 h ("I + D"), and after annealing and hydrothermal exposure of 200 h ("I + A + D").

The crack profile of I + A + D specimens aged for 200 h and tested by flexure is clearly revealed by optical observation of the surface of fracture. A dark zone can be distinguished around the crack (Fig. 6). As will be shown below, this zone corresponds to intergranular fracture and shows high levels of monoclinic content. It can also be appreciated on this fracture surface how, near the indentation imprint, the appearance of the fracture surface of both Palmqvist cracks is also dark but wider than the dark region far from the imprint. This dark zone is usually observed in specimens without any ageing treatment (Fig. 6, left picture). So, in this part of the fracture surface, probably the contrast is due to the degradation effect on the crack front, as happens on the other side of the crack, but also because in the region close the plastic zone fracture is already more intergranular in annealed specimens. The same fracture surface of Fig. 6 was observed by SEM as shown in Fig. 7. Here, at higher magnification, the region seen as dark by optical microscopy is revealed as having intergranular fracture with a small zone formed of crumbled grains. It has a similar appearance to that observed on the specimen surface after degradation (Fig. 7c).

Finally, an I + D specimen (aged for 100 h) was grounded and polished in order to eliminate the degraded layer at the surface, until only a cross-section of the indentation cracks could be observed. Fig. 8 shows an AFM image of the remaining crack profiles. The crack is closed because of removal of residual stresses by grinding. A zone can be clearly appreciated around the crack, which corresponds to the zone affected by the water exposure (this zone has low mechanical integrity and is thus much more affected by the grinding and polishing). The width of the transformed layer at both sides of the crack faces is about 5 μm, but the crack tip radius is smaller.

3.3. Monoclinic content on the fracture surface

Micro-Raman spectra was taken at different positions on the fracture surface of an indented and aged specimen in order to confirm that the region observed around the indentation crack had been transformed. Fig. 9 shows the locations examined and their corresponding spectra. There are large amounts of monoclinic content on the zones affected by the water. On the crack surfaces (point A) including the crack front (points B and D) and on the external surface (C) the thickness of degraded layer and the monoclinic fraction are large enough to produce a strong monoclinic signal. On the other hand, for locations well outside the indentation crack, there is practically no monoclinic content (≈6% in point E corresponding to a measurement in the bulk fracture zone), indicating that during strength testing t–m transformation toughening is nearly negligible as compared to the amount of transformation produced by hydrothermal ageing.

4. Discussion

4.1. Ageing of indented specimens

It is relevant to first analyze the strength of the indented specimens in terms of basic fracture mechanics, in order to properly analyze later the effect of ageing. As the degraded layer was

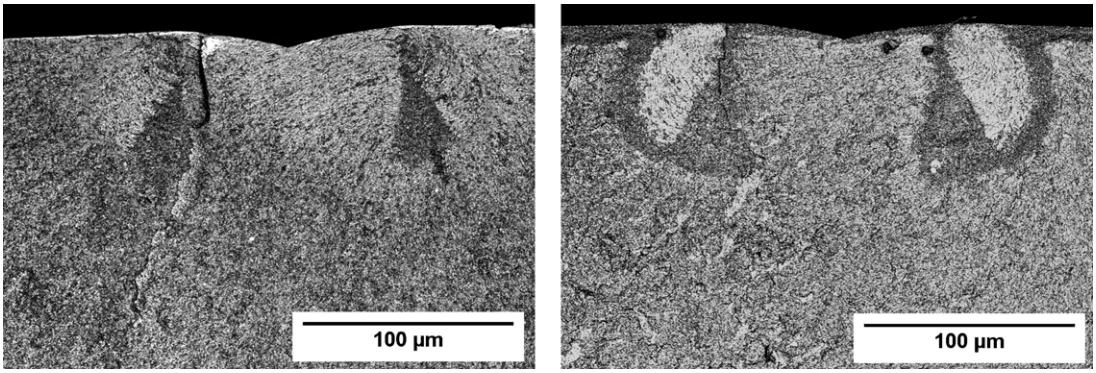

Fig. 6. LSCM images of the fracture surfaces of 10 kg indentation cracks. Both specimens were annealed for 1 h in order to remove the indentation residual stresses around the cracks: (Left) annealed; (Right) annealed and hydrothermally exposed for 200 h.

always significantly smaller than the indentation cracks, fracture in an indented specimen was controlled by the produced cracks. These cracks were much smaller than the specimen size, so it is possible to consider the stress intensity factor of a surface semielliptical crack in a prismatic bar of infinite thickness in order to estimate the strength. For the present crack shape ($a/c \approx 1.9$; a and c are the ellipse semiaxes), the local stress intensity factor is largest at the specimen surface. Therefore, fracture starts at the surface under bending. If we assume that the elliptical shape is maintained, the stress intensity factor at this point increases during crack extension as well as at the deepest point, since a/c diminishes. Therefore, once the crack starts to propagate at the surface, fracture will follow without further increasing the stress. The strength will be given by:

$$\sigma_{ann} = \frac{K_{\mathrm{IC}}}{\psi\,(\phi = 0, a/c = 1.9)\,\sqrt{a}} \tag{4}$$

Considering $a = 64$ μm, the K_{IC} value previously determined, and a factor $\psi(\phi = 0,\ a/c = 1.9) = 1.20$, this equation yields an estimation of 540 MPa. This is reasonably close to the observed 461 ± 44 MPa for a specimen indented and annealed (i.e., with no residual tensions) considering the hypothesis made by using Eq. (4) with the value of K_{IC} obtained from indentation. For example, if only the true K_{IC} were just about 15% lower than the

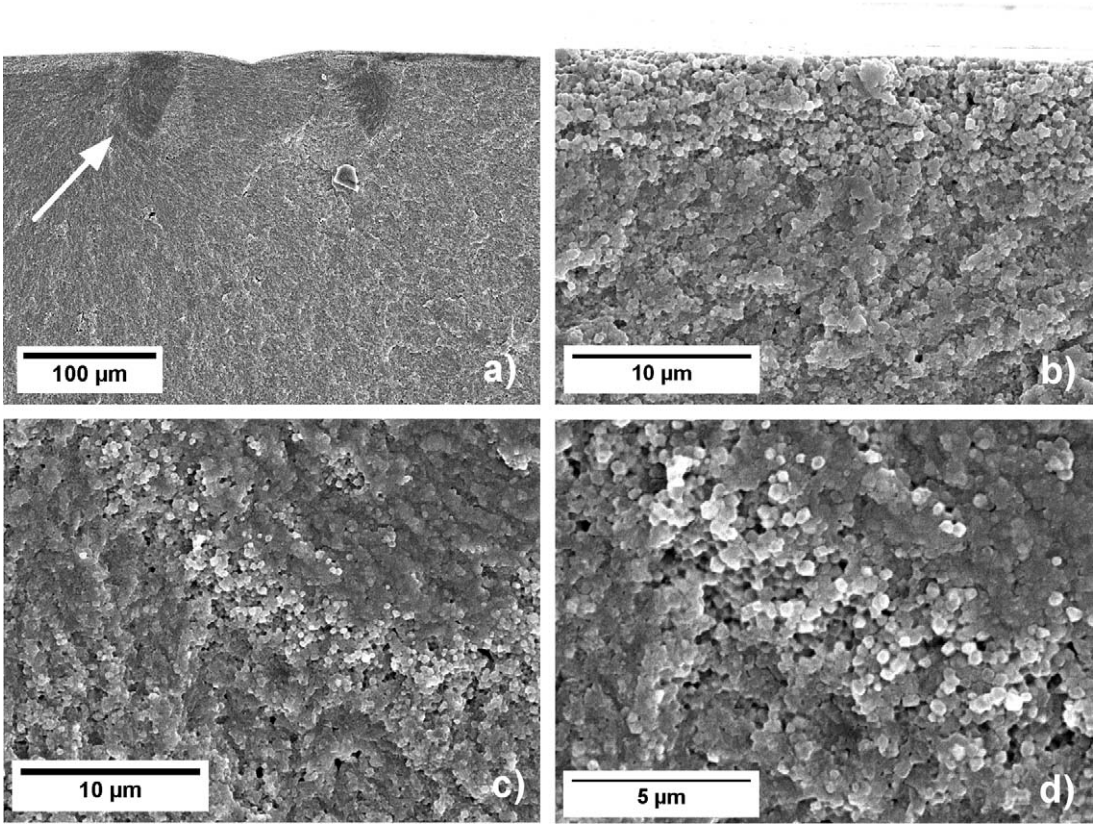

Fig. 7. SEM micrographs of the fracture surface of a I + A + D (200 h): (a) general view of the indentation cracks, (b) degraded layer at the surface of the specimen, (c and d) crumbled micro-cracked degraded zone close to the border of the indentation crack.

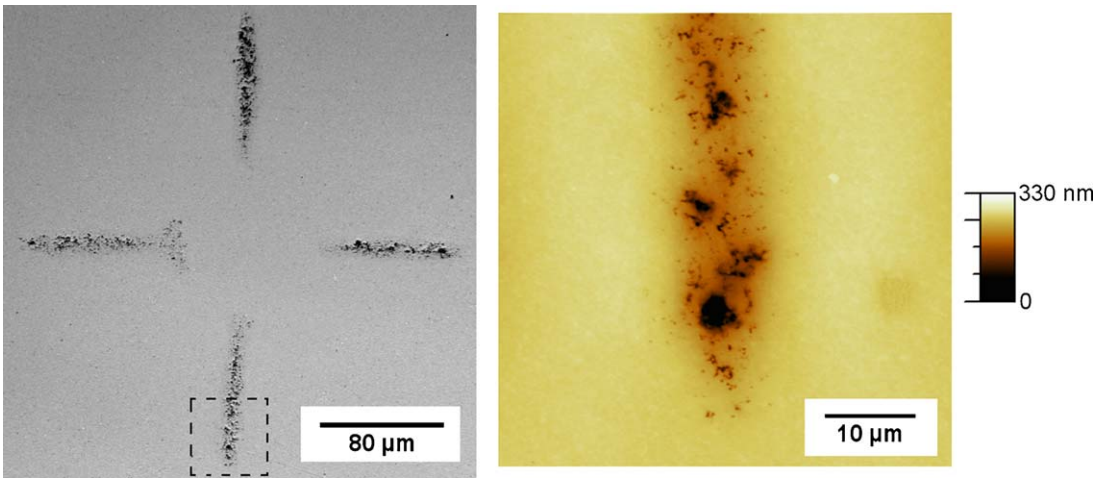

Fig. 8. (Left) LSCM image of indentation cracks degraded for 100 h. After degradation, the specimen surface has been removed by polishing leaving only the crack profiles of the indentation; (Right) AFM image showing one of the crack tips at greater magnification. A damaged area can be appreciated around the crack.

present indentation value, then the present discrepancy would disappear. On the other hand, the calculation uses the original crack dimensions of non-annealed I + D specimens assuming that no crack-bonding took place during annealing. If the effective dimensions of the crack had been reduced by annealing, then expected strength from Eq. (4) would have been even higher that the strength measured increasing this discrepancy.

It is surprising the observed increase of strength with ageing for a specimen with indentation cracks. When the crack faces are in contact with the water vapour they will transform into monoclinic phase for a certain depth similarly as in the specimen surface and a transformed zone will form in front of the crack tip. Fractographic and Raman analysis show the appearance of an intergranular microcracked transformed zone in front of the crack tip when the specimen has been previously degraded. This zone marks clearly the profile of the indentation crack and only appears after ageing. In alumina specimens, Swab and Quinn[26] have found "halos" on the crack periphery as a consequence of environmentally-assisted slow crack-growth. Independently of the exact mechanism, here it is shown that in tetragonal zirconia the marks around the cracks appear systematically as a consequence of ageing (there was no mark in the non-aged specimens).

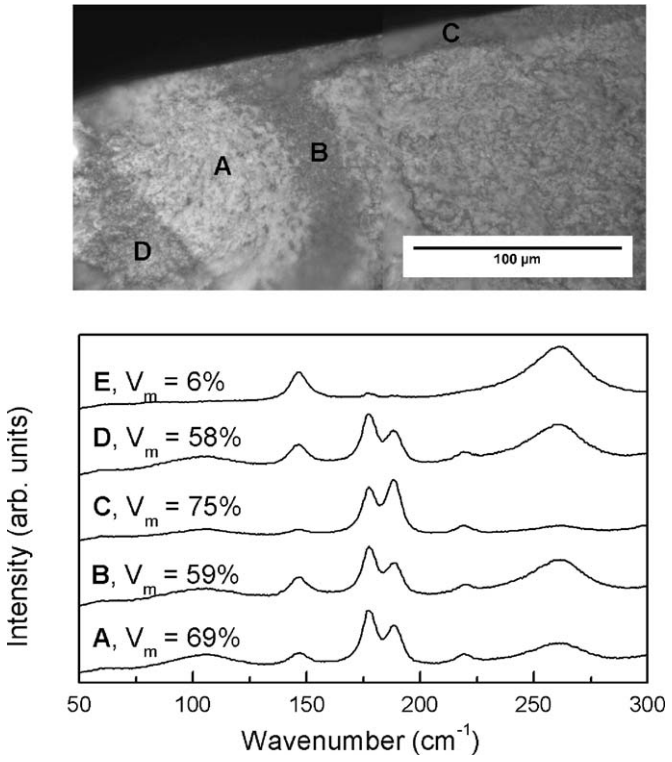

Fig. 9. Raman spectra of different positions on the fracture surface of a specimen with a Palmqvist crack which had been aged. Pattern E was measured 2 mm away from the specimen border.

When bending is applied on an indented and degraded specimen the stress concentrates in front of the crack tip where a highly transformed and microcracked zone of very low strength has been produced by ageing. We believe that under the multiaxial stresses in front of the crack tip, microcrack coalescence takes place at relatively small load and the crack moves forward until it encounters the non-aged material. The crack then stops and tends to deflect parallel to the interface, but the maximum deflection to both sides of the original crack plane is of the order of the thickness of the degraded layer in front of the crack tip. By this mechanism, the crack may get blunted to a radius similar to the degraded layer thickness, producing an increase in strength by crack blunting. The blunted crack tip radius should reach a critical value in order to have a measurable effect on the strength.

The effect of the notch radius in K_{IC} evaluation tests has been widely studied for ceramics. In fact, it is difficult to produce an artificial notch with a radius below 10 µm. The maximum permitted notch radius for a valid K_{IC} evaluation test depends much on the microstructure. In a fine microstructure like the present one, it is reported that true fracture toughness can only be measured when the artificial notch radius is smaller than 3 µm.[19,24] The present work allows observing the change in strength when a sharp crack becomes blunted by hydrothermal ageing. Let's assume that ageing blunts the crack to a radius similar to the

degraded layer thickness, d. The relationship between the stress intensity factors of a blunt and a sharp crack is given by[25]:

$$\frac{K_{IC,blunt}}{K_{Ic}} = \left(1 + \frac{d}{2r_0}\right)^{1/2} \quad (5)$$

where $K_{IC,blunt}$ is the stress intensity factor of the notch at fracture, K_{IC} is the true fracture toughness of the sharp crack, and r_0 represents the size of the fracture process zone ahead of crack tip. Assuming that the observed strength relationship between the I + A + D (blunt crack) and I + A (sharp crack) specimens corresponds to the relationship in Eq. (5), then one obtains $d/r_0 \approx 2.5$ for 200 h of ageing. If the blunted radius corresponds approximately to the affected zone around the crack tip ($d \approx 6\,\mu m$ corresponding to the intergranular region seen by fractography, Fig. 7), then the characteristic distance defined previously is $r_0 \approx 2.4\,\mu m$ for the particular indentation crack considered here, and which is a reasonable value.

For an ageing time shorter than 50 h, the indentation crack is still sharp enough and the fracture strength does not change significantly. For longer times, the effect of crack blunting starts to be reflected in the strength and the extent of blunting can be assessed by the intergranular micro-cracked crumbled region in front of the crack tip. After ageing for 100 h, there is already a clear increase in strength. This means that the degraded layer in front the crack tip is already significant as has been shown in Fig. 8. Degradation ahead of the indentation crack is larger near the specimen surface, because there the material is exposed to water through the specimen surface as well as through the crack surfaces. However, the calculation of the strength from the fracture toughness was carried out only in the annealed non degraded condition for which these effects are absent; the degraded material was used only to determine the crack size. For the ratio of strengths used with Eq. (5), this effect has not been taken into account.

4.2. Ageing of natural defects

It may seem a paradox that LTD reduces the strength of natural crack-like defects in smooth specimens while strengthening specimens with indentation cracks. For commercial 3Y-TZP with strength of 1000 MPa, the critical size for a semicircular surface defect can be simply estimated as having a radius of less than about 17 μm. Actually, critical defects are rather pore agglomerates resulting from the sintering process, which have small cracks and the borders.

For short ageing times, the degraded layer is so thin that its effect will be too small for inducing a significant change in the strength of smooth specimens. For example, for a short ageing time of 24 h, the strength of 3Y-TZP smooth rods decreases only by less than about 5%.[15] However, at longer times, the monoclinic layer becomes thick enough so that fracture may originate not from the original critical natural defects in the non-degraded specimens, but from defects in the degraded layer. These cracks can be initiated from relatively small defects and extend easily under stress in the deep and lateral direction because of the small fracture toughness of the monoclinic phase; they stop when encounter the tetragonal interface in the perpendicular direction. For longer times of ageing, the strength will be controlled by the thickness of the degraded layer and it will drop as this layer becomes thicker. Later on, when the interface does not longer controls the fracture process, this will be governed by the properties of the surface monoclinic layer instead of by natural defects. Therefore, the effect of hydrothermal degradation on cracks can only be observed when there is a large crack that controls the strength.

5. Conclusions

In spite of the decrease in flexural strength that occurs in aged 3Y-TZP, here it is shown that when fracture is controlled by a sharp indentation crack the strength increases significantly with ageing with water vapour. A similar effect can be observed on indented specimens that are previously annealed to eliminate residual indentation stresses. During ageing, an intergranular zone around the indentation crack can be observed by fractography; furthermore this zone shows high monoclinic content. The observed increase in strength can be explained in terms of crack blunting by the degraded and micro-cracked monoclinic zone ahead of the original crack tip which becomes transformed by the influence of water vapour and which is completely surrounded by the high toughness tetragonal phase.

Acknowledgements

The authors gratefully acknowledge the financial support from the Ministerio de Ciencia e Innovación (MICINN) of Spain through project MAT2008-03398 and the research grant given to F. Garcia Marro. The general financial support to the research group given by the Generalitat de Catalunya is also fully acknowledged (2009SGR01285).

References

1. Sergo LV. *Low temperature degradation ageing of zirconia: a critical review of the relevant aspects in dentistry*. *Dent Mater* 2010;**26**:922–8.
2. Green DJ, Hannink JRH, Swain MV. *Transformation toughening of ceramics*. Boca Bacon, FL: CRC Press; 1989.
3. Kobayashi K, Kuwajima H, Masaki T. *Phase change and mechanical properties of ZrO_2–Y_2O_3 solid electrolyte after ageing*. *Solid State Ion* 1980;**3/4**:489–93.
4. Chevalier J, Gremillard L, Deville S. *Low-temperature degradation of zirconia and implications for biomedical implants*. *Ann Rev Mater Res* 2007;**37**:1–32.
5. Clarke IC, Green DD, Pezzotti G, Donaldson D. *20 years experience of zirconia total hip replacements*. *Ceram Orthop Book* 2005;**79**:67–78.
6. Masonis JL, Bourne RB, Ries MD, McCalden RW, Salehi A, Kelman DC. *Zirconia femoral head fractures: a clinical and retrieval analysis*. *J Arthroplasty* 2004;**19**:898–905.
7. Norton MO, Yarlagadda R, Anderson GH. *Catastrophic failure of the Elite Plus total hip replacement, with a Hylamer acetabulum and zirconia ceramic femoral head*. *J Bone Joint Surg B* 2002;**84**:631–5.
8. Tsukuma K, Kubota Y, Tsukidate T. Advances in ceramics, vol. 12. In: Claussen N, Rühle M, Heuer AH, editors. *Science and Technology of Zirconia II*. Columbus, OH: American Ceramic Society; 1984. p. 382.
9. Marro FG, Chintapalli R, Hvizdos P, Soldera F, Mücklich F, Anglada M. *Study of near surface changes in yttria-doped tetragonal zirconia after low temperature degradation*. *Int J Mater Res* 2009;**100**:92–6.

10. Marro FG, Valle J, Mestra A, Anglada M. *Surface modification of 3Y-TZP with cerium oxide*. *J Eur Ceram Soc* 2011;**31**:331–8.
11. Marro FG, Mestra A, Anglada M. *Contact damage in a Ce-TZP/Al_2O_3 nanocomposite*. *J Eur Ceram Soc* 2011;**31**:2189–97.
12. Muñoz-Tabares JA, Jiménez-Piqué E, Anglada M. *Subsurface evaluation of hydrothermal degradation of zirconia*. *Acta Mater* 2011;**59**:473–84.
13. Pajares A, Guiberteau F, Cumbrera FL, Steinbrech RW, Dominguez-Rodriguez A. *Analysis of kidney-shaped indentation cracks in 4Y-PSZ. Acta Mater* 1996;**44**:4387–94.
14. Wang J, Ponton CB, Marquis PM. *The closure of indentation cracks by low temperature degradation*. *Scripta Metall et Mater* 1992;**27**:815–20.
15. Feder A, Anglada M. *Low-temperature ageing degradation of 2.5Y-TZP heat-treated at 1650 °C*. *J Eur Ceram Soc* 2005;**25**:3117.
16. Gaillard Y, Anglada M, Jimenez-Pique E. *Nanoindentation of yttria-doped zirconia. Effect of crystallographic structure on deformation mechanisms*. *J Mater Res* 2009;**24**:719–27.
17. Niihara K, Morena R, Hasselman DP H. *Evaluation of K_{IC} of brittle solids by the indentation method with low crack-to-indent ratios*. *J Mater Sci Lett* 1982;**1**:13–6.
18. Kruzic JJ, Kim DK, Koester KJ, Ritchie RO. *Indentation techniques for evaluating the fracture toughness of biomaterials and hard tissues*. *J Mech Behav Biomed Mater* 2009;**2**:384–95.
19. Damani RJ, Schuster Ch, Danzer R. *Polished notch modification of SENB-S fracture toughness testing*. *J Eur Ceram Soc* 1997;**17**:1685–9.
20. Eichler J, Hoffman M, Eisele U, Rödel J. *R-curve behaviour of 2Y-TZP with submicron grain size*. *J Am Ceram Soc* 2006;**26**:3575–82.
21. Chevalier J, Olagnon C, Fantozzi G. *Study of the residual stress field around Vickers indentations in a 3Y-TZP*. *J Mater Sci* 1996;**31**:2711–7.
22. Katagiri G, Ishida H, Ishitani A, Masaki T. Direct determination by Raman microprobe of the transformation zone size in Y_2O_3 containing tetragonal ZrO_2 polycrystals. In: Somiya S, Yamamoto N, Yanagida H, editors. *Science and Technology of Zirconia III*. Westerville, OH: American Ceramic Society; 1988. pp. 537–44.
23. Chantikul P, Anstis GR, Lawn BR, Marshall DB. *A critical evaluation of indentation techniques for measuring fracture toughness: II: strength method*. *J Am Ceram Soc* 1981;**64**(9):539–43.
24. Damani R, Gstrein R, Danzer R. *Critical notch-root radius effect in SENB-S fracture toughness testing*. *J Eur Ceram Soc* 1996;**16**:695–702.
25. Deng Z-Y, She J, Inagaki Y, Yang J-F, Ohji T, Tanaka Y. *Reinforcement by crack-tip blunting in porous ceramics*. *J Eur Ceram Soc* 2004;**24**(7):2055–9.
26. Swab J, Quinn GD. *Effect of precrack "halos" on fracture toughness determined by the surface crack in flexure method*. *J Am Ceram Soc* 1998;**81**:2261–8.